

Performance Analysis of Different Hybrid Precoding Schemes in 5G mmWave massive MIMO Systems

Md. Mizanul Hoque, Md. Mustafa Kamal, Md. Masud Karim, Md. Kayesh, Sawkat Osman

Abstract— Millimeter-wave (mmWave) communication is most likely to appear as an aspiring technology in the upcoming generation of cellular communication (5G). To confront several challenges (e.g., system complexity, energy consumption, etc.), hybrid precoding is largely investigated in mmWave massive MIMO systems due to its low energy consuming nature and reduced system complexity. The analog processing part of the hybrid precoding network is analyzed by either Phase-Shifters (PS) or Switches (SW) or by Switches and Inverters (SI). In this paper, we consider the downlink communication of a mmWave massive MIMO system and analyze the achievable sum-rate of a hybrid precoding scheme based on successive interference cancellation (SIC) algorithm which utilizes PS, along with two other precoding schemes namely AS-based and ACE-based precoding which utilizes SW and SI respectively in both mmWave channels as well as in different wireless channels. Results demonstrate that the SIC-based scheme achieves near-optimum sum-rate in different wireless channels and mmWave channel as well to other architectures and performs even better in the conventional wireless channels than in mmWave channel. Results also indicate that the sum-rate is even nearer to optimal when the user antennas and RF chains are sufficiently increased.

Index Terms— 5G, massive MIMO, mmWave, hybrid precoding, achievable sum-rate, near-optimal.

1 INTRODUCTION

CISCO Internet Business Solutions Group (IBSG) predicted that there will be 50 billion connected devices by the year 2020 [1]. To handle this huge wireless data traffic, current cellular technology (e.g., fourth generation) is most likely to be replaced by 5G technology [2]. The spectrum abundance in mmWave frequencies (30-300 GHz) has led it to be a 'gold rush' technology in the development of 5G. Another aspiring technology of 5G is massive MIMO which essentially assembles transmitter and receiver antennas to ensure better sum-rate [3]. To recover few shortcomings of mmWave communication associated with its small wavelength and severe path loss, more advanced technology has been proposed recently: unification of mmWave and massive MIMO [4] which has the potential to achieve higher sum-rate associated with massive MIMO configuration and large antenna array gain associated with a high frequency of mmWave communication, hence can greatly mitigate the serious attenuation problem in mmWave communication. Hybrid analog/digital precoding [5] has been introduced recently for its potential to lower both cost and complexity of the system because of using reduced RF chains, which is also very feasible in mmWave massive MIMO net-

works. In the analog RF processing part of hybrid precoding, largely three types of networks have been analyzed: the first one is the finite precision variable PS-based architecture which works by altering the phases of the complex symbols at the baseband, the second one is SW-based architecture [6] which reduces the cost and power consumption to a great extent and the third one is switch and inverter (SI)-based net architecture which works by altering the phases of the complex symbols at the baseband, the second one is SW-based architecture work [7]. To increase the achievable sum-rate as much as possible (near-optimal), the authors of [8] have developed a SIC-based hybrid precoding scheme (PS-based), where they disintegrate whole capacity optimization problem into two sub-classes; every sub-class considers a sub-array and then capacity optimization of each sub-array is performed sequentially. In this work, we exploit the SIC-based scheme and evaluate its achievable sum-rate and compare it with the sum-rate of AS-based and ACE-based hybrid precoding [7] in different wireless channels and mmWave channel as well with different massive MIMO antenna configurations. The main contribution of this paper is the analysis of the sum-rate of SIC-based precoding in different channels.

In Section 2, system model is introduced. In Section 3, simulation results are discussed. Lastly in Section 4, the conclusion is drawn.

2 SYSTEM MODEL

Figure 1 depicts hybrid precoding architecture for downlink mmWave massive MIMO communication. The base station (BS) supports N antennas and NRF RF chains to provide K users. Now the receive signal vector y for K users is expressed as:

$$y = H F_{RF} F_{BS} s + n \quad (1)$$

- Author Md. Mizanul Hoque has completed MSc. in ICT from, Bangladesh University of Professionals. Dhaka, Bangladesh. E-mail: mizan.ruetete08@yahoo.com
- Co-Author Md. Mustafa Kamal has completed MSc. in ICT from, Bangladesh University of Professionals. Dhaka, Bangladesh. E-mail: mustafa2319@gmail.com
- Co-Author Md. Masud karim is pursuing MSc. in EEE from, Bangladesh University of Engineering & Technology. Dhaka, Bangladesh. E-mail: masudkarim521@yahoo.com
- Co-Author Md. Kayesh has completed BSc. in ETE from, Rajshahi University of Engineering & Technology. Rajshahi, Bangladesh. E-mail: kayesh.ete.ruet@gmail.com
- Co-Author Sawkat Usman has completed BSc. in ETE from, Rajshahi University of Engineering & Technology. Rajshahi, Bangladesh. E-mail: sawkat.144048@gmail.com

where H is the channel matrix, F_{BB} denotes baseband digital precoder with dimension $N_{RF} \times K$ satisfying the total transmit power constraint as $\|F_{RF}F_{BB}\|_F^2 = \gamma$, where γ is the total transmit power and n is the additive white Gaussian noise (AWGN) vector which follows independent and identical distribution (i.i.d.) $CN(0, \sigma^2)$. Now, the achievable sum-rate R can be expressed as:

$$R = \log_2(1 + SINR_k) \tag{2}$$

Where, $SINR_k$ represents the signal-to-interference-plus-noise ratio of the k^{th} user which can be obtained from (14) in [7]. The channel matrix H is obtained from (2) in [7], where they obtained the geometric channel model for mmWave communications. Now, this channel matrix H can be derived for different wireless channels also. The Rayleigh fading channel can be modeled as [9]:

$$H_{(rayleigh)} \sim CN(0, \sigma^2) \tag{3}$$

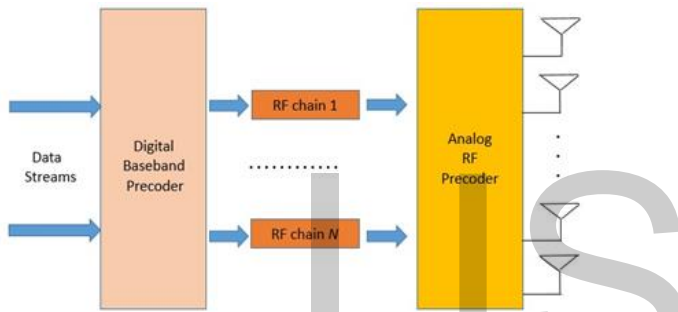


Fig. 1: Hybrid precoding structure for mmWave massive MIMO systems.

with circularly symmetric complex Gaussian random variables. The Rician fading channel can be modeled as [9]:

$$H_{(rician)} = \sqrt{\frac{k}{k+1}} \sigma e^{j\theta} + \sqrt{\frac{1}{k+1}} CN(0, \sigma^2) \tag{4}$$

where the first term corresponds to the specular path arriving with uniform phase θ and the second term corresponding to the aggregation of the large number of reflected and scattered paths, independent of θ . The parameter k (Rician factor) is the ratio of the energy in the specular path to the energy in the scattered paths.

The Nakagami- m fading channel can be written as [10]:

$$H_{(nakagami-m)} = G e^{j\theta} \tag{5}$$

Where,

$$G = (G_{Re}^2 + G_{Im}^2)^{\frac{1}{2}} \tag{6}$$

and θ is defined as $(0, 2\pi)$.

Z_{Re}^2 is a Chi-square distributed random number, which is given by,

$$Z_{Re}^2 = X_1^2 + X_2^2 + \dots + X_m^2 \tag{7}$$

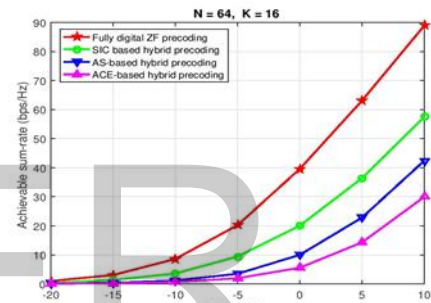
Where, X_i is the m -Gaussian random variables with zero mean and variance $\frac{2}{m}$ in both the real and imaginary parts.

$$x \sim N(0, \frac{1}{\sqrt{2m}})$$

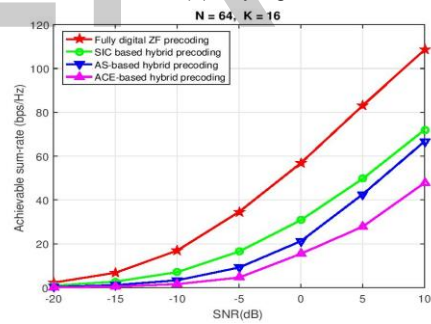
3 SIMULATION RESULTS

3.1 Sum-rate vs SNR

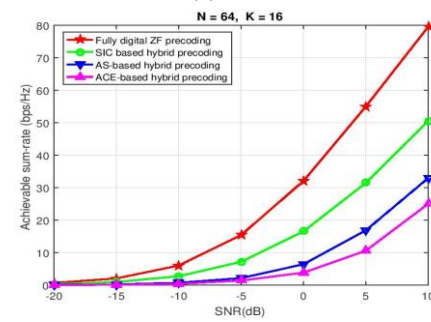
Figure 2 evaluates the SE comparison in Rayleigh, Rician, and Nakagami- m fading channels respectively, where $N = 64$ and $K = 16$. Here the SIC-based scheme is for PS based architecture, AS-based precoding is based on SW-based network and the ACE-based hybrid precoding is for Si-based architecture [7]. In Fig. 2a, for the Rayleigh fading channel, we observe that the SIC-based scheme outperforms other precoding schemes (except the ZF precoding) in terms of SE. The best performance of digital ZF precoding is only intuitive as it enables only digital precoder for precoding purposes. For the Rayleigh fading channel, we notice the SIC-based hybrid precoding exceeds SE of the AS-based scheme by 4 dB and ACE-based scheme by almost 6 dB. The same trend is followed in Fig. 2b, for



(a) Rayleigh

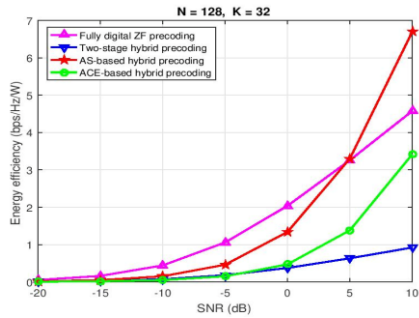


(b) Rician

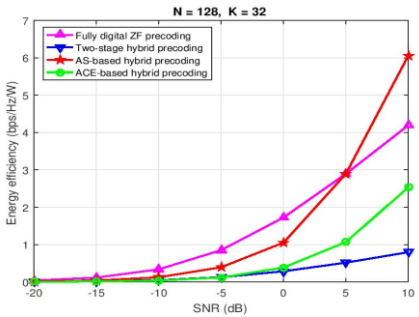


(c) Nakagami-m

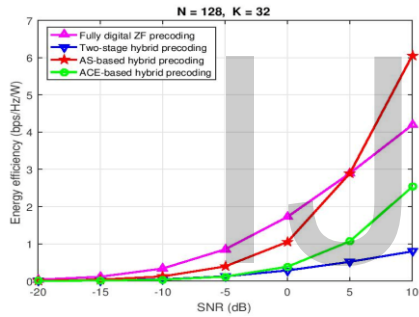
Fig. 2: Achievable sum-rate comparison, where $N = 64$ and $K = 16$ for (a) Rayleigh fading channel, (b) Rician fading channel, (c) Nakagami- m fading channel.



(a) Rayleigh



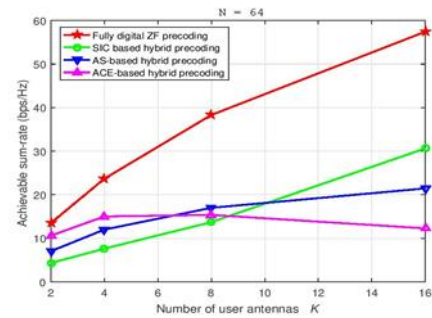
(b) Rician



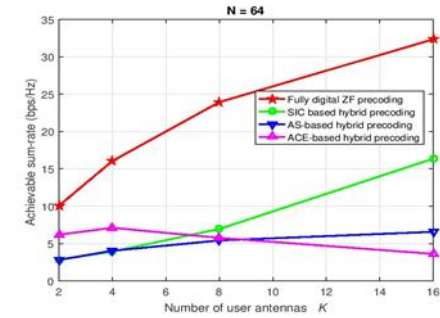
(c) Nakagami-m

Fig. 3: Achievable sum-rate comparison, where $N = 128$ and $K = 32$ for (a) Rayleigh fading channel, (b) Rician fading channel, (c) Nakagami-m fading channel.

Rician channel but the SE is greater here than for Rayleigh channel. The gap between the curves has also shrunk noticeably. The reason behind the increased SE in the Rician channel is that the Rician channel has at least one strong line-of-sight (LoS) path while transmission of signals, as a result, the achievable sum-rate is higher here. For Nakagami-m fading channel in Fig. 2c, the same trend is observed as the Rayleigh fading channel. In all 3 channels, the reason behind the high SE of SIC-based hybrid precoding is that it utilizes a high number of phase-shifters in the analog processing part of precoding while the AS-based scheme utilizes energy-efficient switches for the same purpose and the ACE-based scheme uses even more energy-efficient switches and inverters, as a result, their achievable sum-rate is much lower in all the channels than SIC-based hybrid precoding. In Fig. 3, for $N = 128$ and $K = 32$, the same trend is followed throughout the whole SNR range by the schemes in all 3 channels as in Fig. 2 except for the fact that the SE of all the methods increased almost double as a result of increased base station antennas and user



(b) Rician



(c) Nakagami-m

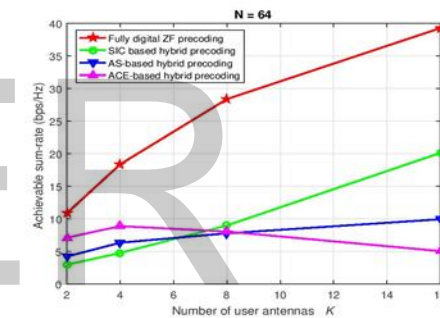


Fig. 4: Achievable sum-rate comparison against K , where $N = 64$ for (a) Rayleigh fading channel, (b) Rician fading channel, (c) Nakagami-m fading channel.

antennas.

3.2 Sum-rate vs K

In Fig. 4, the achievable sum-rate comparison against K is shown in the same channels as in Fig. 2 and in Fig. 3 where $N = 64$ and K is varied from 1 to 16. Here we observe the digital ZF precoding performs best as earlier. And the SIC-based scheme achieves a higher sum-rate than other schemes particularly after $K \geq 8$, there is a linear upward curve of the SIC-based scheme as K increases. We also observe that the ACE-based precoding suffers severe degradation after $K \geq 8$ which in turn implies that as the number of users increases to a certain level, the AS and ACE-based scheme fails to provide with sufficient sum-rate while the SIC-based precoding achieves sufficient sum-rate even with an increased number of users since it utilizes a large number of phase-shifters in the analog processing part. Here also the highest sum-rate is observed in the Rician channel. Figure 5 illustrates the sum rate comparison when $N = 128$ and K is varied from 1 to 32. Here the SIC-based schemes achieve higher sum-rate than other schemes particularly after $K \geq 8$. And the sum-rate is also in-

creased much more as a result of the increased number of base station antennas.

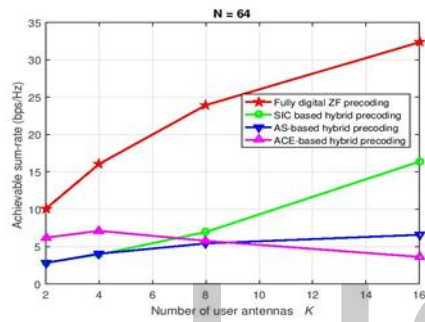
3.3 Sum-rate analysis in mmWave channel

Figure 6 evaluates the SE comparison for different massive MIMO antenna configurations in the mmWave channel. In Fig. 6a, when $N = 16, K = 4$, we observe a higher sum-rate of ACE-based precoding than other schemes, which is interesting to notice. This is because as the number of base station antennas and users is very limited here, the ACE-based scheme can achieve sufficient sum-rate throughout the SNR range. Then again in Fig. 6b, the higher sum-rate of the old SICbased scheme is observed when $N = 64$ and $K = 16$. Here we notice that the achievable sum-rate of the SIC-based scheme is 48 bps/Hz whereas, for the same antenna configuration ($N = 64, K = 16$), the sum-rate is much higher in Rayleigh, Rician, and

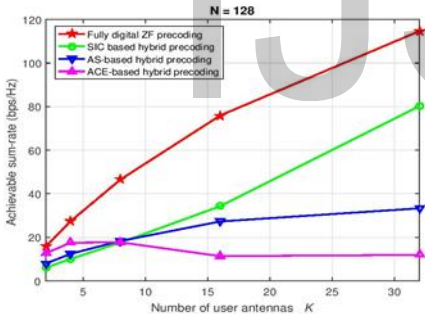
TABLE 1
SIMULATION PARAMETERS

Parameter	Notation	Value
K	Number of user antennas	4, 16, 32
N	Number of BS antennas	16, 64, 128
r	Number of channel realizations	1000
F	Carrier frequency (mmWave channel)	28 GHz
L	Number of effective path (mmWave channel)	3
m	Shape factor of Nakagami-m fading channel	5
k	Rician factor	5

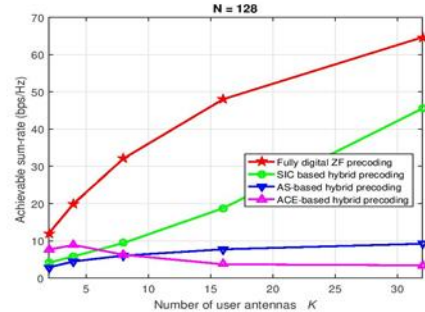
This goes for the other schemes as well. In Fig. 6c, the same trend is noticed for $N = 128$ and $K = 64$.



(a) Rayleigh



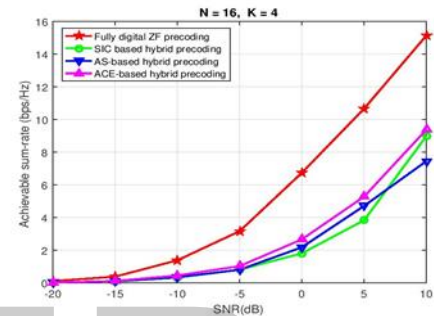
(b) Rician



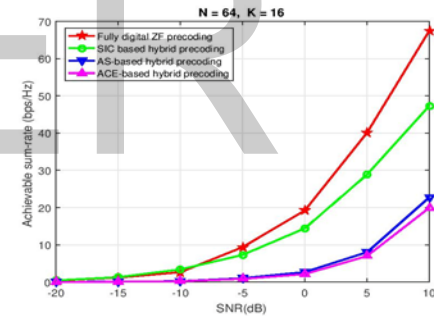
(c) Nakagami-m

Fig. 5: Achievable sum-rate comparison against K, where $N = 128$ for (a) Rayleigh fading channel, (b) Rician fading channel, (c) Nakagami-m fading channel.

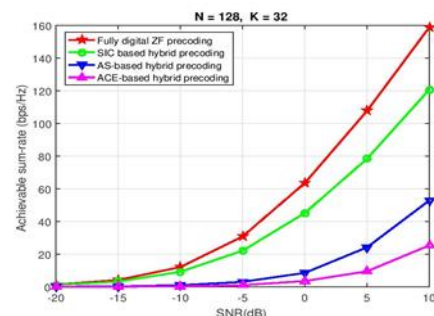
Nakagami-m fading channels (58,67 and 51 bps/Hz respectively).



(a) Rayleigh



(b) Rician



(c) Nakagami-m

Fig. 6: Achievable sum-rate comparison for mmWave channel.

Figure 7 illustrates the sum-rate comparison against K in mmWave channel. In Fig. 7a, we observe the better performance of ACEbased schemes. than other precoding methods which are again since there is a very limited number of N and K. When $N = 64$ and K is varied from 1 to 16 we again observe

the higher sum-rate performance of the SIC-based scheme where the AS and ACE-based precoding suffers poorly along with the range of K. In Fig.7c, the same trend is observed. The reason behind the higher sum-rate in conventional wireless channels than in mmWave channel is that the mmWave channel has very limited multipath components and poor scattering nature compared to the i.i.d. Rayleigh fading and other conventional channels.

future work will focus on analyzing the energy efficiency of these hybrid precoding methods in the mmWave channel as well as in different wireless channels.

ACKNOWLEDGMENT

The authors wish to thank Dr. Md. Manjure Mowla, associate Professor, Electronics & Telecommunication Engineering, RUET.

REFERENCES

- [1] D. Evans, "The internet of things: How the next evolution of the internet is changing everything," CISCO white paper, vol. 1, no. 2011, pp. 1-11, 2011.
- [2] W. Roh, J.-Y. Seol, J. Park, B. Lee, J. Lee, Y. Kim, J. Cho, K. Cheun, and F. Aryanfar, "Millimeter-wave beamforming as an enabling technology for 5g cellular communications: Theoretical feasibility and prototype results," IEEE communications magazine, vol. 52, no. 2, pp. 106-113, 2014.
- [3] E. G. Larsson, O. Edfors, F. Tufvesson, and T. L. Marzetta, "Massive mimo for next generation wireless systems," IEEE communications magazine, vol. 52, no. 2, pp. 186-195, 2014.
- [4] T. E. Bogale and L. B. Le, "Massive mimo and mmwave for 5g wireless hetnet: Potential benefits and challenges," IEEE Vehicular Technology Magazine, vol. 11, no. 1, pp. 64-75, 2016.
- [5] L. Liang, W. Xu, and X. Dong, "Low-complexity hybrid precoding in massive multiuser mimo systems," IEEE Wireless Communications Letters, vol. 3, no. 6, pp. 653-656, 2014.
- [6] R. Mendez-Rial, C. Rusu, A. Alkhateeb, N. Gonzalez-Prelcic, and R. W. Heath, "Channel estimation and hybrid combining for mmwave: Phase shifters or switches?" in 2015 Information Theory and Applications Workshop (ITA). IEEE, 2015, pp. 90-97.
- [7] X. Gao, L. Dai, Y. Sun, S. Han, and I. Chih-Lin, "Machine learning inspired energy-efficient hybrid precoding for mmwave massive mimo systems," in 2017 IEEE International Conference on Communications (ICC). IEEE, 2017, pp. 1-6.
- [8] X. Gao, L. Dai, S. Han, I. Chih-Lin, and R. W. Heath, "Energy-efficient hybrid analog and digital precoding for mmwave mimo systems with large antenna arrays," IEEE Journal on Selected Areas in Communications, vol. 34, no. 4, pp. 998-1009, 2016.
- [9] D. Tse and P. Viswanath, Fundamentals of wireless communication. Cambridge university press, 2005.
- [10] E. Pakdeejit, "Linear precoding performance of massive mu-mimo downlink system," 2013. L. Hubert and P. Arabie, "Comparing Partitions," J. Classification, vol. 2, no. 4, pp. 193-218, Apr. 1985. (Journal or magazine citation)

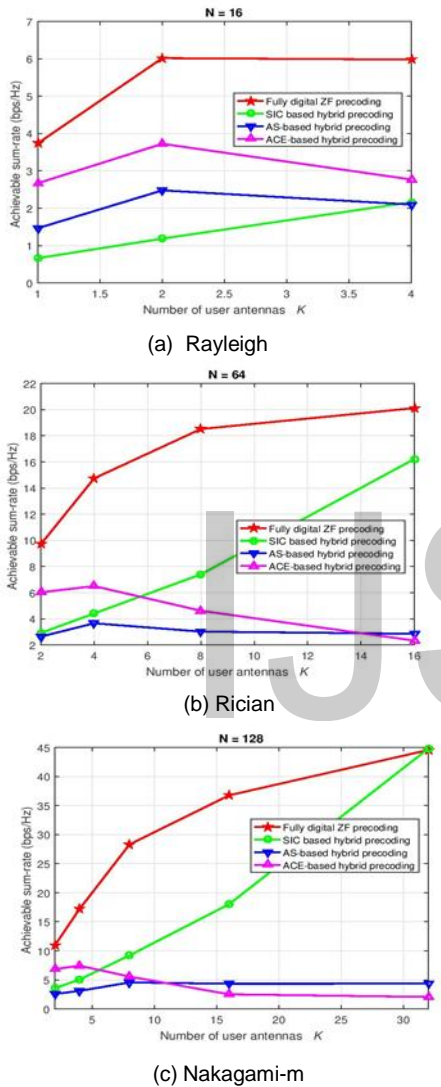


Fig. 7: Achievable sum-rate comparison against K for mmWave channel.

4 CONCLUSION

In this paper, we analyze various hybrid precoding schemes in various wireless channels. Simulation results depict that the SIC-based hybrid precoding enjoys near-optimal achievable sum-rate in both mmWave channel and different wireless channels since it utilizes a high number of phase-shifters and performs even better in the conventional wireless channels than in mmWave channel. Results also indicate that the achievable sum-rate can be made even closer to optimal by increasing the number of user antennas and RF chains. Our